

1 **Evaluation of cation exchange membrane performance under exposure to high Hg⁰ and**
2 **HgBr₂ concentrations**

3 Matthieu B. Miller¹, Sarrah M. Dunham-Cheatham², Mae Sexauer Gustin², Grant C. Edwards^{1,†}

4 ¹Faculty of Science and Engineering, Department of Environmental Sciences, Macquarie University, Sydney, NSW,
5 2109, Australia

6 ²Department of Natural Resources and Environmental Science, University of Nevada, Reno NV, 89557, United
7 States

8 [†]Deceased 10 September 2018

9

10 Correspondence to: Mae Sexauer Gustin mgustin@cabnr.unr.edu

11 **Abstract**

12 Reactive mercury (RM), the sum of both gaseous oxidized Hg and particulate bound Hg, is an
13 important component of the global atmospheric mercury cycle, but measurement currently
14 depends on un-calibrated operationally-defined methods with large uncertainty and demonstrated
15 interferences and artifacts. Cation exchange membranes (CEM) provide a promising alternative
16 methodology for quantification of RM, but method validation and improvements are ongoing.

17 For the CEM material to be reliable, uptake of gaseous elemental mercury (GEM) must be
18 negligible under all conditions, and RM compounds must be captured and retained with high
19 efficiency. In this study, the performance of CEM material under exposure to high
20 concentrations of GEM (1.43×10^6 to 1.85×10^6 pg m⁻³) and reactive gaseous mercury bromide
21 (HgBr₂ ~ 5000 pg m⁻³) was explored, using a custom-built mercury vapor permeation system.

22 Quantification of total permeated Hg was measured via pyrolysis at 600 °C and detection using a
23 Tekran® 2537A. Permeation tests were conducted for 24 to 72 hours in clean laboratory air, with
24 absolute humidity levels ranging from 0.1 to 10 g m⁻³ water vapor. GEM uptake by the CEM
25 material averaged no more than 0.004% of total exposure for all test conditions, which equates to
26 a non-detectable GEM artifact for typical ambient air sample concentrations. Recovery of HgBr₂
27 on CEM filters was >100 % compared to calculated total permeated HgBr₂ based on the
28

30 downstream Tekran® 2537A data. These results suggest incomplete thermal decomposition due
31 to the pyrolyzer or the gold trap in the Tekran 2537, as the CEM demonstrated a high collection
32 efficiency for HgBr₂, as indicated by less than 1% downstream breakthrough on average.

33

34 **1 Introduction**

35 Mercury (Hg) is a persistent environmental contaminant with a significant atmospheric life time,
36 and the form and chemistry of Hg is an important determinant of its biogeochemical cycling.
37 Mercury in the atmosphere is found in three forms: gaseous elemental mercury (GEM), gaseous
38 oxidized mercury (GOM), and particulate bound mercury (PBM). PBM and GOM are often
39 quantified together as reactive mercury (RM = GOM + PBM). Atmospheric GEM, at an average
40 global background concentration of 1 to 2 ng m⁻³, can be reliably measured with calibrated
41 analytical instruments (Gustin et al., 2015; Slemr et al., 2015). The measurement of GOM and
42 PBM requires detection at part per quadrillion (pg m⁻³) concentrations, and depends currently on
43 un-calibrated operationally defined methods with demonstrated interferences and artifacts, and
44 concomitant large uncertainty (Maruszczak et al., 2017; Jaffe et al. 2014; McClure et al. 2014;
45 Gustin et al. 2013; Lyman et al. 2010). Recent reviews (Zhang et al., 2017; Gustin et al., 2015)
46 detail the shortcomings, difficulties, developments, and ongoing improvements for atmospheric
47 RM measurements.

48 One alternative methodology that may provide improved measurement of ambient RM involves
49 use of cation exchange membranes (CEM). CEM materials have been used to selectively
50 measure GOM concentrations in ambient air in previous studies (Huang et al., 2017; Maruszczak
51 et al., 2017; Pierce and Gustin, 2017; Huang and Gustin, 2015a; Huang et al., 2013; Sheu and
52 Mason, 2001; Ebinghaus et al., 1999; Mason et al., 1997; Bloom et al., 1996). Use of CEM type
53 filters (then manufactured by Gelman Sciences and referred to as “ion exchange membranes”)

54 for this purpose was first documented in the literature in a conference presentation (Bloom et al.,
55 1996), though these had also been deployed in an earlier field-based international comparative
56 study of RM measurement techniques in September, 1995 (Ebinghaus et al., 1999). In the
57 comparative study, one participating lab deployed a series of ion exchange membranes (for
58 GOM) behind a quartz fiber filter (for PBM) at a sample flow rate of 9 to 10 Lpm, for 24 h
59 measurements (filter pore sizes were not reported). Results for PBM and GOM were in similar
60 ranges of 4.5 to 26 pg m^{-3} and 13 to 23 pg m^{-3} , respectively (Ebinghaus et al., 1999).

61 The ion exchange membrane method was also applied in a 1995-96 field campaign for
62 determining the speciation of atmospheric Hg in the Chesapeake Bay area (Mason et al., 1997).
63 This study used a 5-stage Teflon filter pack system that included one up front quartz fiber filter
64 (0.8 μm pore size) to remove particles, and four downstream Gelman ion exchange membranes
65 (pore size not reported) to 1) capture GOM, 2) capture GOM breakthrough, 3) serve as
66 deployment blanks, and 4) isolate the filter train on the downstream side (Mason et al., 1997).
67 Concentrations of GOM were reported to be 5-10 pg m^{-3} , essentially at or below the method
68 detection limit and it was speculated that even this small amount may have been an artifact from
69 fine particulate Hg passing through the 0.8 μm quartz fiber filter (Mason et al., 1997). These low
70 concentrations are likely due to GOM being degraded on the quartz fiber filter or inefficient
71 uptake by the Gelman filter (see Supplemental Information Gustin et al. 2013). The 3rd-in-series
72 ion exchange membrane blanks were reported to be not significantly different in Hg
73 concentration from unused membrane material, indicating that breakthrough was not a
74 phenomenon that extended past the second ion exchange filter position.

75 The particulate Hg artifact problem was subsequently elaborated on in a further comparative
76 study focusing exclusively on RM measurement techniques (Sheu and Mason, 2001). Specific
77 concerns included physical particle breakthrough, re-evolution of gas-phase Hg^{2+} from PBM

78 captured on the upstream particulate filters passing downstream to the ion exchange membranes,
79 possible adsorption of GOM compounds to the particulate filters, or a GEM collection artifact on
80 the ion exchange membranes. None of these concerns were proven or disproven conclusively.

81 Recent CEM based sampling systems typically deploy a pair of CEM disc filters without a pre-
82 particulate filter, in replicates of 2 to 3 at a flow rate of 1.0 Lpm (Gustin et al., 2016). Each pair
83 of filters constitutes one sample, the first filter serving as the primary RM collection surface, and
84 the second filter capturing breakthrough. Filters are deployed for 1 to 2 weeks and then collected
85 for analysis (Huang et al., 2017). The CEM material consists of a negatively charged
86 polyethersulfone coated matrix (Pall Corporation), and at least one manufacturing evolution has
87 occurred (Huang and Gustin, 2015b). Prior CEM material versions (I.C.E. 450) had a pore size
88 of 0.45 μm , while the current CEM material (Mustang[®] S) has a manufacturer reported pore size
89 of 0.8 μm .

90 Previous work with the I.C.E 450 material indicated it does not adsorb significant quantities of
91 GEM in passive exposures, but selectively uptakes gas-phase Hg^{2+} species (Lyman et al., 2007).
92 The CEM material was subsequently adapted for use in active sample flow systems, with the
93 presumption of continued inertness to GEM and selectivity for GOM (Huang and Gustin, 2015a;
94 Huang et al., 2013). These studies and others (Lyman et al., 2016) have shown better GOM
95 recovery on CEM material compared to potassium chloride (KCl) coated denuder methods.

96 Despite these tests, the transparency of the CEM material to GEM uptake has not been
97 conclusively demonstrated for active sampling flow rates, nor for high GEM concentrations,
98 though limited data using low concentration manual Hg^0 injections through CEM filters suggests
99 little or no GEM uptake (Lyman et al., 2016). However, even small rates of GEM uptake by the
100 CEM material could result in a significant measurement artifact (e.g. a modest 1 to 2% GEM

101 uptake could easily overwhelm detection of typical ambient GOM concentrations). It is therefore
102 important that a GEM artifact be ruled out if the CEM material is to be successfully deployed for
103 ambient RM measurements.

104 Additionally, previous studies observed significant amounts of “breakthrough” GOM on the
105 secondary filter. The amount of breakthrough is not consistent, neither as a constant mass, with
106 total Hg ranging from zero to as high as 400 pg (Huang et al., 2017), nor as a percentage of Hg
107 collected on the primary filter, ranging from 0 to 40% (Pierce and Gustin, 2017). Similar variable
108 breakthrough issues were observed in the earliest field-based CEM measurements as well
109 (Mason et al., 1997). In contrast to ambient measurements, previous laboratory experiments have
110 reported only minor (0 to 16%) or no breakthrough Huang and Gustin, 2015a; Huang et al.,
111 2013). Limited experimental work with flow rates of 1.0 and 16.7 Lpm in ambient air could not
112 provide an explanation for differing breakthrough rates (Pierce and Gustin, 2017).

113 In this research we investigated the potential for GEM uptake on CEM material using a custom-
114 built permeation system. Tests were done to investigate the ability of a pyrolyzer to convert
115 GEM to GOM. In addition, the ability of the CEM material to capture and retain a
116 representative GOM compound (mercury(II) bromide, $HgBr_2$) was explored, and the collection
117 efficiency for this compound was estimated. we attempted explain or rule out possible
118 mechanisms of RM breakthrough for both dry and humid conditions.

119

120

121

122

123 **2 Methods**

124 **2.1 System for sampling configuration**

125 A Tekran® 2537A ambient mercury analyzer was integrated with a custom-built permeation
126 system designed to enable controlled exposures of GEM and GOM to CEM filters (Fig. 1). The
127 2537A analyzer was calibrated at the beginning and periodically throughout the study and
128 checked for accuracy by manual Hg⁰ injections (mean recovery 101.1% ± 4.3, n = 10, SI Fig. 1).
129 The entire system was checked for Hg contamination in clean air prior to permeation tests, and
130 periodically during sampling (SI Fig. 1). See SI for additional information on Tekran quality
131 control. All tubing and connections used in the permeation system were polytetrafluoroethylene
132 (PTFE), except for the quartz glass pyrolyzer tube and perfluoroalkoxy (PFA) filter holders.
133 Given its reactive nature, some GOM inevitably adsorbs to internal line surfaces, but the capacity
134 of these materials to sorb and retain GOM is not infinite and a steady state of
135 adsorption/desorption is expected after 5-6 hours of exposure to a stable concentration (Xiao et
136 al., 1997;Gustin et al., 2013).

137 Sample flow through the system was alternated between two PTFE sample lines (designated
138 Line 0 and Line 1) using a Tekran® Automated Dual Switching (TADS) unit. Sample air was
139 constantly pulled through each line at 1.0 Lpm by the internal pump and mass flow controller
140 (MFC) in the 2537A, or by an external flush pump (KNF Laboport® N86 KNP) and MFC (Sierra
141 Smart-Trak® 2). Laboratory air was pulled through a single inlet at the combined rate of 2.0
142 Lpm, passing through a 0.2 µm PTFE particulate filter and an activated charcoal scrubber
143 (granular activated carbon 6-12 mesh, FisherChemical®) to produce clean sample air.
144 Additionally, for dry air permeations sample air was pulled through a Tekran® 1102 Air Dryer
145 installed upstream of the particulate filter, and for elevated humidity permeations sample air was

146 pulled through the headspace of a distilled water bath (DIW, < 0.2 ng L⁻¹ total Hg) that was
147 located upstream from the charcoal scrubber to eliminate the DIW being a potential Hg source to
148 the system. Temperature and relative humidity (RH) were measured in-line (Campbell Scientific
149 CS215) and used for calculation of absolute humidity.

150 Pure liquid Hg⁰ and crystalline HgBr₂ (purity > 99.998% Sigma-Aldrich[®]) were used as Hg
151 vapor sources. The elemental Hg⁰ bead was contained in a PTFE vial. Solid HgBr₂ crystals were
152 packed in thin-walled PTFE heat-shrink tubing (O.D. 0.635 cm) with solid Teflon plugs in both
153 ends to create a perm tube with an active permeation length of 2 mm (Huang et al., 2013). The
154 HgBr₂ permeation tube was also placed in the bottom of a PTFE vial, and the permeation vials
155 were submerged in a temperature-controlled laboratory chiller (0.06 ± 0.13 °C, Cole Parmer
156 Polystat[®]). A low source temperature was favored, because higher temperatures would have
157 produced unacceptably high concentrations, and there is evidence that at higher temperatures a
158 small amount of Hg⁰ can be evolved from Hg²⁺ compounds (Xiao et al., 1997).

159 An ultra-high purity nitrogen (N₂) carrier gas was passed through the permeation vials at 0.2
160 Lpm to carry the target Hg vapor into the main sample line through a PTFE T-junction. The main
161 sample line was split into Line 0 and Line 1 immediately downstream from the permeation flow
162 junction, with flow on each line controlled by MFC. Line 0 proceeded directly to the 2537A
163 without modification during GEM permeations (Fig. 1A), but housed CEM filters during the
164 HgBr₂ permeations (Fig. 1B, 1C). Line 1 contained an in-line pyrolyzer unit. The goal of the
165 pyrolyzer was to convert all Hg to GEM for detection on the Tekran[®] 2537A.

166 2.2 Pyrolyzer

167 The pyrolyzer used in the study (SI Fig. 3) consisted of a 25.4 cm long quartz glass tube of 0.625
168 cm diameter (custom, URG Corporation). A loosely packed 3 cm section of quartz wool was

169 lodged in the mid-section of the tube, and this 3 cm section was wrapped with 22 gauge
170 Nichrome wire (18 loops). The quartz tube was closely contained within 2.5 cm thick quartz
171 fiber insulation within a 1.6 mm aluminum casing, except for an enclosed air space around the
172 heated Nichrome coil section. The coil wire was connected to 16 AWG stranded copper wire
173 with all metal disconnects that were buried within the quartz fiber insulation to reduce thermal
174 fatigue on the connections. The copper wire insulation was stripped and replaced with higher
175 temperature heat-shrink insulation where the wiring passed through the pyrolyzer case to the
176 external power supply. The tip of a 150 mm long K-type thermocouple (Auber WRNK-191) was
177 inserted through the insulation into the heated air space next to the coil to provide a temperature
178 feedback for a PID controller (Auber SYL-1512A). Power to the Nichrome coil was supplied by
179 a 12 VDC transformer through a solid-state relay (Auber MGR-1D4825) switched by the PID
180 controller. It was found that the position of the feedback thermocouple in the airspace outside of
181 the heating coil caused a large discrepancy between nominal temperature setpoint and actual
182 temperature inside the heated section of pyrolyzer tube. In general, much higher temperatures are
183 achieved inside the coil than outside. To compensate for this, actual temperature at the heated
184 coil section was verified to 600°C by external IR sensor and internal thermocouple probe.

185 To test if higher pyrolyzer temperatures converted more GOM to GEM for detection by the
186 Tekran 2537, the pyrolyzer temperature was increased to 650, 800, and 1,000°C (SI Fig. 4).
187 Pyrolyzer temperatures were measured by placing a thermocouple inside the pyrolyzer. GOM
188 concentrations measured as GEM by the Tekran 2537 increased at 600 and 800°C relative to
189 375°C. There was no significant difference between the amount of mercury concentrations in the
190 downstream Tekran 2537 when the pyrolyzer was at 600 and 800°C (*t-test*, $p = 0.08$),
191 indicating that the increased pyrolyzer temperature did not convert more GOM to GEM.
192 However, when the pyrolyzer temperature was increased to 1000 °C, significantly more mercury

193 was measured by the downstream Tekran 2537 relative to when the pyrolyzer was at 650°C (t -
194 *test*, $p = 0.00$), indicating that the higher temperature was more efficient at converting GOM to
195 GEM; however, the pyrolyzer design could not sustain the 1000 °C temperature and was deemed
196 unsafe to use in the experimental permeation system. Thus, all experiments were performed with
197 a pyrolyzer temperature of 600°C.

198 The residence time in the pyrolyzer tube was approximately 1.5 seconds. Quartz wool was added
199 to increase the amount of surface area available to facilitate reactions and maximize the amount
200 of GOM converted to GEM in the pyrolyzer. Because of the conversion rate (discussed below),
201 this is a pretty efficient method for converting GOM to GEM. Having an efficient pyrolyzer
202 provides us with a means of constraining perm tube permeation rates.

203

204 **2.3 Sample deployment**

205 CEM filters were deployed in 2-stage, 47 mm disc PFA filter holders (Savillex[©]). The primary
206 “A” filter in the 2-stage holder is the first to be exposed to the permeated Hg, with the secondary
207 “B” filter mounted immediately behind the A filter (A to B distance ~ 3mm) to measure potential
208 breakthrough. For GEM permeations, three 2-stage filter holders were placed in-series on Line 1
209 behind the pyrolyzer unit (Fig. 1A), while total Hg coming through the system was measured on
210 Line 0 with no filters in place. This allowed simultaneous exposure of 6 CEM filters in one GEM
211 sample exposure. The first CEM filter in-line served to scrub any small residual RM passing
212 through the system and pyrolyzer, and these first in-line filters were removed for the calculations
213 of mean GEM uptake rate, (SI. 5 and discussion). A controlled experiment was also performed to
214 ensure that both Lines 0 and 1 were conducting comparable concentrations of mercury under the
215 experimental conditions. Two-stage filter packs were deployed with CEM filters in each line at
216 equal distances from the permeation tube. The membranes were deployed for the same amount

217 of time in triplicate and analyzed to quantify the amount of total mercury sorbed to the
218 membranes. The average % deviation between lines was 2.9%, with a maximum deviation of
219 5.4%. These results indicated that though there may be some difference in the amount of
220 mercury passing through Lines 0 and 1, the difference was relatively small.

221 For determining the potential for GOM breakthrough, two system configurations were used. In
222 the first configuration (Fig. 1B), the total Hg concentration of air that passed through the
223 pyrolyzer on Line 1 was measured without any filters, while Line 0 held one 2-stage CEM filter
224 pair for HgBr₂ loading. This configuration allowed for 10 min interval quantification of the
225 HgBr₂ permeation concentration through Line 1 using the 2537A, and comparison with total Hg
226 loading on the CEM filters on Line 0.

227 In the second configuration, replicate filters were concurrently loaded with HgBr₂ by placing 2-
228 stage CEM filter holders on both Line 0 and Line 1 (upstream of the pyrolyzer, Fig. 1C). In all
229 HgBr₂ exposures, the filter holders were placed as close to the permeation vial as possible, with a
230 total distance from vial to filter surface of approximately 20 cm. Mercury bromide permeation
231 was conducted in dry air and elevated humidity air. The difference between one line being fully
232 open to the HgBr₂ permeation flow (configuration Fig. 1B) and then closed by deployment of the
233 CEM filters (configuration Fig. 1C) enabled a rough determination of the amount of HgBr₂ line-
234 loss within the system.

235 **2.4 Analyses of cation exchange membranes**

236 After permeation, CEM filters were collected into clean, sterile polypropylene vials and analyzed
237 for total Hg by digestion in an oxidizing acid solution, reduction to Hg⁰, gold amalgamation, and
238 final quantification by cold vapor atomic fluorescence spectrometry (CVAFS, EPA Method
239 1631, Rev. E) using a Tekran® 2600 system. The system background Hg signal was determined

240 for every analytical run by analyzing pure reagent solution in the same vials and at the same
241 volume as used for actual filter samples. Total Hg standards (5 to 100 ppb) were analyzed before
242 and after each batch of 10 filter samples to check precision and recovery, and the mean recovery
243 for all Hg standards was $97.2 \pm 5.0\%$ ($n = 37$). Analysis for total Hg on the CEM filters
244 provided for comparison of total Hg filter loading, and verification of in-line results. A to B filter
245 breakthrough was calculated by comparison of total Hg recoveries on the primary and secondary
246 CEM filters, using Eq. (1):

247
$$\% \text{ Breakthrough} = 100 * \text{CEM}_{2nd} / (\text{CEM}_{1st} + \text{CEM}_{2nd}) \quad (1)$$

248 Blank CEM filters were collected and analyzed in the same manner with every set of sample
249 filters deployed on the permeation system, and the overall mean filter blank value was subtracted
250 from all total Hg values to calculate the final blank-corrected Hg values used for data analysis.
251 All data were analyzed in Microsoft® Excel (version 16.12) and RStudio® (version 3.2.2).

252 **3 Results**

253 **3.1 Elemental Mercury Uptake on CEM Filters**

254 Elemental Hg uptake on CEM material was negligible for permeated Hg^0 vapor concentrations
255 ranging from 1.43×10^6 to $1.85 \times 10^6 \text{ pg m}^{-3}$ (Fig. 2). High GEM concentrations were employed in
256 this study under the logic that if no GEM uptake was observed at high concentrations, a similar
257 lack of GEM uptake can be expected for lower concentrations.

258 The mean Hg mass on blank CEM filters was $50 \pm 20 \text{ pg}$ ($n = 28$). For permeations into dry
259 sample air of $0.5 \pm 0.1 \text{ g m}^{-3}$ water vapor (WV), total mean Hg^0 permeation exposures of 2.7×10^6
260 pg (24 h) and $7.3 \times 10^6 \text{ pg}$ (72 h) resulted in total (blank-corrected) Hg recoveries on the CEM
261 filters of $100 \pm 40 \text{ pg}$ ($n = 10$) and $280 \pm 110 \text{ pg}$ ($n = 5$), respectively. These quantities of total

262 recovered Hg equate to a mean GEM uptake rate on the CEM filters of $0.004 \pm 0.002\%$ ($0.006 \pm$
263 0.006% including first in-line filter). For GEM permeations into ambient humidity sample air (2
264 to 4 g m^{-3} WV), at a slightly lower total mean permeated Hg^0 24 h exposure of $2.1 \times 10^6 \text{ pg}$, total
265 (blank-corrected) Hg recoveries on the CEM filters were $55 \pm 30 \text{ pg}$ ($n = 10$), equating to a GEM
266 uptake rate of $0.003 \pm 0.001\%$ ($0.005 \pm 0.005\%$ including first in-line filter).

267 The first CEM filter in line during the GEM permeations always showed more total Hg than the
268 following 5 downstream filters, which were not significantly different from each other (SI Fig.
269 5). It is unlikely that the Hg observed on the first CEM filters resulted from GEM uptake. Even
270 at the highest GEM permeation rate, the first filter captured only $\sim 1700 \text{ pg}$ of Hg, out of a total
271 permeated amount of over *7.3 million pg* (a 0.02 % uptake rate). This means that the downstream
272 CEM filters were still exposed to about *7.2985 million pg* of GEM but captured less total Hg. As
273 we cannot entirely rule out the possibility of some small rate of *in-situ* oxidation of GEM in the
274 system, at the surface of the Hg^0 bead or in the vapor phase, the first in-line filters were not
275 included in the calculation of GEM uptake rates because of suspicion that some component of
276 the Hg captured on the first filter was GOM. Inclusion or removal of the first in-line filters did
277 not significantly alter calculations.

278 The overall GEM uptake rate was linear ($r^2 = 0.97$, $p = 0.0004$) for the range of concentrations
279 used in this study, indicating a similar low uptake rate can be expected down to lower GEM
280 concentrations.

281

282

283

284 **3.2 Mercury Bromide Uptake on CEM Filters**

285 Breakthrough of HgBr_2 vapor from the primary (A) to secondary (B) CEM filters was low for all
286 conditions tested in this study (Table 1). These conditions included HgBr_2 permeated into clean
287 dry laboratory air with $< 0.5 \text{ g m}^{-3}$ WV, clean air at ambient room humidity (4 to 5 g m^{-3} WV),
288 and clean air at elevated humidity (10 to 11 g m^{-3} WV), at line temperatures between 17 to 19
289 $^{\circ}\text{C}$. Overall, the mean A to B filter breakthrough ranged from 0 to 0.5%, and averaged 0.2 ± 0.2
290 % ($n = 17$), with no statistical difference observed in mean breakthrough rates for the three levels
291 of humidity (ANOVA, $p = 0.124$).

292 The first HgBr_2 permeation in clean dry ($< 0.5 \text{ g m}^{-3}$ WV) laboratory air was over a 96 h period,
293 using the system configuration in Fig. 1B to establish an approximate permeation rate (Fig. 3).
294 Total Hg reaching the 2537A through the pyrolyzer on Line 1 (red line, Fig. 3) indicated an
295 average HgBr_2 exposure concentration of 4540 pg m^{-3} , or about 4.5 pg min^{-1} from the permeation
296 tube. This permeated concentration of HgBr_2 was deliberately much higher than ambient in order
297 to test retention and break through at high levels. It should be noted that these concentrations are
298 50 – 1000 times above background ambient concentrations and the performance of the CEM
299 filters at low concentrations could be slightly different. After this permeation, total blank-
300 corrected HgBr_2 loading on the primary CEM filter on Line 0 was 49400 pg, but only 50 pg on
301 the secondary CEM filter, indicating a breakthrough rate of approximately 0.1%. Total Hg
302 reaching the 2537A through the CEM filters on Line 0 (black line, Fig. 3) over this time period
303 was 15 pg, mostly at the beginning of the deployment when some ambient Hg entered the
304 opened system. The low concentrations of Hg measured downstream in Line 0 on the 2537A
305 corroborates that breakthrough of HgBr_2 was low. These data also demonstrate that the CEM
306 material did not saturate with a HgBr_2 loading of $\sim 50000 \text{ pg}$, a loading far higher than could be
307 expected in ambient conditions.

308 Subsequent replicate 24 h HgBr_2 permeations in clean dry air resulted in consistent total Hg
309 loading on CEM filters placed on both lines concurrently ($8560 \pm 320 \text{ pg}$, $n = 6$, Samples 2-7
310 Table 1), and mean total Hg on the secondary CEM filters was $20 \pm 10 \text{ pg}$ (average
311 breakthrough of 0.3%). On Line 0 (black line, Fig.3), which was never open to HgBr_2 vapor
312 downstream from the CEM filters at any point in the study, Hg measured at the 2537A was zero
313 for all three 24 h permeations, indicating no breakthrough (Samples 2, 4, & 6, Table 1).
314 However, on Line 1, which had been exposed to the full HgBr_2 vapor concentration of 4540 pg
315 m^{-3} over the duration of the 96 h perm test, 1155 pg of Hg were measured downstream in the first
316 24 h sample (Sample 3, Table 1). The amount of downstream Hg dropped to 10 pg in the second
317 24 h, and 6 pg in the third 24 h (Samples 5 & 7, Table 1). This downstream Hg in Line 1
318 (compared to the zero Hg simultaneously observed on Line 0) is attributed to volatilization of
319 HgBr_2 that had adsorbed to the line material during the open permeation flow. At the moment
320 CEM filters were deployed on Line 1 (red-to-blue transition, Fig. 3), a rapid asymptotic decline
321 in the Hg signal began. This decay curve supports drawdown and depletion of a Hg reservoir on
322 the interior line surfaces behind the CEM filters, and not a continuous source such as
323 breakthrough from the permeation tube that was still supplying HgBr_2 to both sample lines. The
324 total mass of Hg volatilized from the interior line surfaces (1155 pg) represents 4 to 5% of the
325 total HgBr_2 that had passed through Line 1 ($\sim 25000 \text{ pg}$ based on 2537A measurement).
326 Eventually, Hg reaching the 2537A through Line 1 decreased to zero during the same 24 h filter
327 deployment, indicating the majority of HgBr_2 line contamination in a high-concentration
328 permeation system can be expected to flush out within $\sim 12 \text{ h}$. However, we caution that
329 materials used in high-concentration permeation systems, despite being flushed out, should not
330 be used for background ambient air work without at least a very thorough acid cleaning.

331 Additional HgBr₂ permeations were made at two levels of in-line humidity. At ambient room
332 humidity (4 to 5 g m⁻³ WV), mean total Hg measured on the CEM filters was 7910 ± 520 pg (n =
333 4; Samples H2-5, Table 1), with an average breakthrough to the secondary filters of 0.3%. When
334 normalized for sample volume, the mean HgBr₂ loading on CEM filters during ambient humidity
335 (5968 ± 125 pg) and dry air (5995 ± 188 pg) permeations was not statistically significantly
336 different (t-test *p* = 0.790). HgBr₂ breakthrough rates were also the same (0.3%) as during the
337 dry air permeations, indicating that the permeation system was operating similarly at the two
338 humidity levels, and suggesting that absolute humidity concentrations of 4 to 5 g m⁻³ WV had
339 insignificant effects on collection of HgBr₂ in clean laboratory air by the CEM material.

340 An increase in humidity resulted in an initial large increase in Hg measured at the 2537A
341 downstream of the CEM filters on Line 0 (Sample H1, Table 1), concurrently with an open
342 HgBr₂ permeation flow through Line 1 while both lines were subjected to increased RH. This
343 downstream Hg on Line 0 dropped substantially to zero in ~10 h in the first 24 h deployment
344 (Sample H2, Table 1), and was zero for the duration of the second 24 h deployment (Sample H4,
345 Table 1). Hg rapidly declined to zero, due to off-gassing from the tubing induced by the
346 increased humidity, which facilitated a heterogeneous surface reduction of HgBr₂ to GEM in the
347 short section of line between the perm source and CEM filters. This phenomenon was also
348 observed during the Reno Atmospheric Mercury Intercomparison eXperiment (RAMIX; Gustin
349 et al., 2013). Reduced HgBr₂ then then passed through to the 2537A as GEM. As the
350 breakthrough rate and the mean HgBr₂ loading on the CEM filters did not change between the
351 dry air and ambient humidity permeations, the downstream Hg observed at the 2537A during the
352 ambient humidity permeations cannot be attributed to a loss of Hg from the CEM filters and is
353 more likely due to a process in the sample lines.

354 As a further test of possible humidity effects, two replicate 24 h CEM filter deployments were
355 conducted in elevated humidity conditions (10 to 11 g m⁻³ WV) created by an in-line water bath.
356 Mean total Hg loading on the primary CEM filters was higher compared to the previous
357 permeations (11700 ± 720 pg, n = 4, Samples H9-12, Table 1), indicating an increase in the
358 effective HgBr₂ permeation rate, possibly due to the perturbation caused by a poor filter seal and
359 small leak in the preceding deployment (Sample H7-8, Table 1). However, mean total Hg on the
360 secondary CEM filters was 20 ± 20 pg, indicating an average breakthrough of 0.1%, less than the
361 breakthrough observed for the lower humidity permeations.

362 **4 Conclusions**

363 GEM uptake on the CEM material was negligible under the laboratory conditions and high GEM
364 loading rates (3 orders of magnitude above ambient) tested in this study, with an overall linear
365 uptake rate of 0.004% (SI Fig. 5). This uptake rate would be insignificant at typical ambient
366 atmospheric Hg concentrations (1 to 2 ng m⁻³). As a hypothetical example, a CEM filter
367 sampling ambient air at an average GEM concentration of 2 ng m⁻³ for a typical 2-week sample
368 period would have a total Hg⁰ exposure of ~40000 pg. At the calculated uptake rate of 0.004%, a
369 maximum 1.6 pg of Hg observed on the sample filter could be attributed to GEM artifact. Given
370 that blank filters have a mean total Hg mass of 50 ± 20 pg, this amount would be below the
371 detection limit. This corroborates the lack of GEM uptake seen by Lyman et al. (2016) for
372 manual Hg⁰ injections on CEM filters at lower total mass loadings of 300 to 6000 pg.

373 Mean HgBr₂ breakthrough from primary to secondary CEM filters averaged 0.2 ± 0.2% over all
374 test conditions. A to B filter breakthrough was derived from a comparison between the large
375 amount of HgBr₂ permeated onto the primary CEM filters, to the small amount of HgBr₂ that
376 collected on the secondary CEM filters, 3 mm immediately downstream. The measurement of

377 1000s of pg of Hg on the primary filter, and only 10s of pg on the secondary filter, leads to the
378 conclusion that the primary filter removed the majority of HgBr₂ from the sample air stream
379 under laboratory conditions applied in this study. In addition, low breakthrough was corroborated
380 by downstream measurement of the air stream passing through the CEM filters, using the
381 Tekran® 2537A. The average breakthrough to the 2537A was 0 pg for 24 h permeations in dry
382 air, and 0 to 40 pg in humid air, for filter deployments at steady-state (> 24 h without large
383 perturbations).

384 While the permeation system was not specifically optimized for a quantitative mass balance
385 between permeated HgBr₂ and HgBr₂ recovered on the CEM filters, a rough estimation of the
386 CEM collection efficiency is possible. Using the HgBr₂ permeations conducted in clean dry air
387 (mean loading 8560 pg) and comparing this to the mean Hg concentration measured at the
388 2537A analyzer during the last 24 h of the 96 h permeation measurement (4680 pg m⁻³ or 6739
389 pg per 24 h), HgBr₂ recovery on the CEM filters averaged 127%. Adjusting the expected
390 permeated HgBr₂ mass for our estimated line-loss (~4-5%) changed the recoveries to ~123%.
391 Still, HgBr₂ loading on the CEM filters was ~23% higher than expected based on the pyrolyzed
392 total measurement on the 2537A, indicating not all HgBr₂ was converted to GEM. This can be
393 explained by the pyrolyzer design used in this study not being 100% efficient at thermally
394 reducing HgBr₂ to Hg⁰, based on the higher total Hg recoveries on the CEM filters versus total
395 Hg measured through the pyrolyzer on the Tekran 2537.

396 The technique of gold amalgamation in general, and specifically including the Tekran® 2537
397 analyzer, is widely considered to provide a quantitative total gaseous Hg measurement, at or very
398 near 100% collection efficiency for Hg⁰ and Hg compounds (Temme et al., 2003; Landis et al.,
399 2002; Schroeder et al, 1995; Dumarey et al., 1985; Schroeder and Jackson, 1985). However, to
400 our knowledge collection and desorption efficiencies on gold traps have not been demonstrated

401 for HgBr₂. The stated desorption temperature of the Tekran® 2537A gold traps is 500 °C, but
402 temperatures as low as 375 °C have been reported (Gustin et al., 2013). This would cause
403 reduced thermal decomposition efficiency for all captured GOM compounds, including HgBr₂.
404 We speculate that a combination of incomplete thermal decomposition to Hg⁰ at both the 600 °C
405 pyrolyzer and during the best-case 500 °C desorption of the 2537 gold traps, contributed to the
406 ~20% non-detection of total permeated HgBr₂ as it passed through the CVAFS optical path.

407 While our results validated some basic performance metrics for the CEM material, they did not
408 provide data that could fully explain the higher levels of breakthrough observed for CEM filters
409 deployed in ambient air over the 1-to-2 week sample periods in previous studies. Increasing
410 humidity by itself did not affect observed HgBr₂ breakthrough. A HgBr₂ loading of ~50000 pg
411 also did not lead to increased breakthrough, indicating there is no saturation effect on CEM filter
412 capacity at a GOM loading far greater than expected from ambient concentrations. It remains
413 unclear, though, whether breakthrough results from different collection efficiencies for GOM
414 compounds other than HgBr₂, or whether breakthrough results from a degradation of GOM
415 retention capacity in the CEM material when exposed to ambient air chemistries not simulated in
416 this study. Also, our experiments were conducted in particulate-free air, which leaves open the
417 possibility that breakthrough is related to capture (or lack thereof) of PBM by the CEM material.

418 Further testing and refinements are necessary, beginning with optimization of the pyrolyzer
419 parameters (e.g., temperature, volume) to allow for a more accurate quantitative comparisons
420 between the CEM and Tekran® 2537 results. Permeation rates of HgBr₂ were variable and need
421 to be more precisely controlled, a standardized and stable GOM permeation system being needed
422 in general. This study was undertaken using controlled laboratory conditions, but CEM
423 performance needs to be further validated in ambient air. Specifically, the reasons for RM
424 breaking through CEM filters deployed in ambient air still need to be determined.

425 **Acknowledgements**

426 The authors would like to acknowledge funding from Macquarie University iMQRES 2015148
427 and NSF Grant 629679. Valuable input and assistance were received from Dr. Ashley Pierce, Dr.
428 Seth Lyman, and the students of Dr. Gustin's laboratory. We bid an untimely farewell to Dr.
429 Grant C. Edwards, who was ever a cheerful friend, mentor, and colleague. Dr. Edwards passed
430 away unexpectedly on September 10, 2018.

431

432 **References**

433

434 Bloom, N., Prestbo, E., and VonderGeest, E.: Determination of atmospheric gaseous Hg(II) at
435 the pg/m³ level by collection onto cation exchange membranes, followed by dual
436 amalgamation/cold vapor atomic fluorescence spectrometry, 4th International Conference on
437 Mercury as a Global Pollutant, Hamburg, 1996.

438 Dumarey, R., Dams, R., and Hoste, J.: Comparison of the collection and desorption efficiency of
439 activated charcoal, silver, and gold for the determination of vapor phase atmospheric mercury,
440 Analytical Chemistry, 57, 2638-2643, 10.1021/ac00290a047, 1985.

441 Ebinghaus, R., Jennings, S. G., Schroeder, W. H., Berg, T., Donaghy, T., Guentzel, J., Kenny,
442 C., Kock, H. H., Kvietkus, K., Landing, W., Muhleck, T., Munthe, J., Prestbo, E. M.,
443 Schneeberger, D., Slemr, F., Sommar, J., Urba, A., Wallschlager, D., and Xiao, Z.: International
444 field intercomparison measurements of atmospheric mercury species at Mace Head, Ireland,
445 Atmospheric Environment, 33, 3063-3073, 1999.

446 Gustin, M. S., Huang, J., Miller, M. B., Peterson, C., Jaffe, D. A., Ambrose, J., Finley, B. D.,
447 Lyman, S. N., Call, K., Talbot, R., Feddersen, D., Mao, H., and Lindberg, S. E.: Do We
448 Understand What the Mercury Speciation Instruments Are Actually Measuring? Results of
449 RAMIX, Environmental Science & Technology, 47, 7295-7306, 10.1021/es3039104, 2013.

450 Gustin, M. S., Amos, H. M., Huang, J., Miller, M. B., and Heidecorn, K.: Measuring and
451 modeling mercury in the atmosphere: a critical review, Atmos. Chem. Phys., 15, 5697-5713,
452 10.5194/acp-15-5697-2015, 2015.

453 Gustin, M. S., Pierce, A. M., Huang, J., Miller, M. B., Holmes, H. A., and Loria-Salazar, S. M.:
454 Evidence for Different Reactive Hg Sources and Chemical Compounds at Adjacent Valley and
455 High Elevation Locations, Environmental Science & Technology, 50, 12225-12231,
456 10.1021/acs.est.6b03339, 2016.

457 Huang, J., Miller, M. B., Weiss-Penzias, P., and Gustin, M. S.: Comparison of Gaseous Oxidized
458 Hg Measured by KCl-Coated Denuders, and Nylon and Cation Exchange Membranes,
459 Environmental Science & Technology, 47, 7307-7316, 10.1021/es4012349, 2013.

460 Huang, J., and Gustin, M. S.: Uncertainties of Gaseous Oxidized Mercury Measurements Using
461 KCl-Coated Denuders, Cation-Exchange Membranes, and Nylon Membranes: Humidity
462 Influences, Environmental Science & Technology, 49, 6102-6108, 10.1021/acs.est.5b00098,
463 2015a.

464 Huang, J., and Gustin, M. S.: Use of Passive Sampling Methods and Models to Understand
465 Sources of Mercury Deposition to High Elevation Sites in the Western United States,
466 Environmental Science & Technology, 49, 432-441, 10.1021/es502836w, 2015b.

467 Huang, J., Miller, M. B., Edgerton, E., and Sexauer Gustin, M.: Deciphering potential chemical
468 compounds of gaseous oxidized mercury in Florida, USA, Atmos. Chem. Phys., 17, 1689-1698,
469 10.5194/acp-17-1689-2017, 2017.

470 Jaffe, D. A., Lyman, S., Amos, H. M., Gustin, M. S., Huang, J., Selin, N. E., Levin, L., ter
471 Schure, A., Mason, R. P., Talbot, R., Rutter, A., Finley, B., Jaeglé, L., Shah, V., McClure, C.,
472 Ambrose, J., Gratz, L., Lindberg, S., Weiss-Penzias, P., Sheu, G.-R., Feddersen, D., Horvat, M.,
473 Dastoor, A., Hynes, A. J., Mao, H., Sonke, J. E., Slemr, F., Fisher, J. A., Ebinghaus, R., Zhang,
474 Y., and Edwards, G.: Progress on Understanding Atmospheric Mercury Hampered by Uncertain
475 Measurements, *Environmental Science & Technology*, 48, 7204-7206, 10.1021/es5026432,
476 2014.

477 Landis, M. S., Stevens, R. K., Schaedlich, F., and Prestbo, E. M.: Development and
478 characterization of an annular denuder methodology for the measurement of divalent inorganic
479 reactive gaseous mercury in ambient air, *Environmental Science & Technology*, 36, 3000-3009,
480 10.1021/es015887t, 2002.

481 Lyman, S., Jones, C., O'Neil, T., Allen, T., Miller, M., Gustin, M. S., Pierce, A. M., Luke, W.,
482 Ren, X., and Kelley, P.: Automated Calibration of Atmospheric Oxidized Mercury
483 Measurements, *Environmental Science & Technology*, 50, 12921-12927,
484 10.1021/acs.est.6b04211, 2016.

485 Lyman, S. N., Gustin, M. S., Prestbo, E. M., and Marsik, F. J.: Estimation of Dry Deposition of
486 Atmospheric Mercury in Nevada by Direct and Indirect Methods, *Environmental Science &*
487 *Technology*, 41, 1970-1976, 10.1021/es062323m, 2007.

488 Lyman, S. N., Jaffe, D. A., and Gustin, M. S.: Release of mercury halides from KCl denuders in
489 the presence of ozone, *Atmospheric Chemistry and Physics*, 10, 8197-8204, 10.5194/acp-10-
490 8197-2010, 2010.

491 Maruszczak, N., Sonke, J. E., Fu, X., and Jiskra, M.: Tropospheric GOM at the Pic du Midi
492 Observatory—Correcting Bias in Denuder Based Observations, *Environmental Science &*
493 *Technology*, 51, 863-869, 10.1021/acs.est.6b04999, 2017.

494 Mason, R., Lawson, N., and Sullivan, K.: The concentration, speciation and sources of mercury
495 in Chesapeake Bay precipitation, *Atmospheric Environment*, 31, 3541-3550, 10.1016/S1352-
496 2310(97)00206-9, 1997.

497 McClure, C. D., Jaffe, D. A., and Edgerton, E. S.: Evaluation of the KCl Denuder Method for
498 Gaseous Oxidized Mercury using HgBr₂ at an In-Service AMNet Site, *Environmental Science &*
499 *Technology*, 48, 11437-11444, 10.1021/es502545k, 2014.

500 Pierce, A. M., and Gustin, M. S.: Development of a Particulate Mass Measurement System for
501 Quantification of Ambient Reactive Mercury, *Environmental Science & Technology*, 51, 436-
502 445, 10.1021/acs.est.6b04707, 2017.

503 Schroeder, W., and Jackson, R.: An instrumental analytical technique for speciation of
504 atmospheric mercury, *International Journal of Environmental Analytical Chemistry*, 22, 1-18,
505 10.1080/03067318508076405, 1985.

506 Schroeder, W., Keeler, G., Kock, H., Roussel, P., Schneeberger, D., and Schaedlich, F.:
507 International field intercomparison of atmospheric mercury measurement methods, Water Air
508 and Soil Pollution, 80, 611-620, 10.1007/BF01189713, 1995.

509 Sheu, G. R., and Mason, R. P.: An examination of methods for the measurements of reactive
510 gaseous mercury in the atmosphere, Environmental Science & Technology, 35, 1209-1216,
511 10.1021/es001183s, 2001.

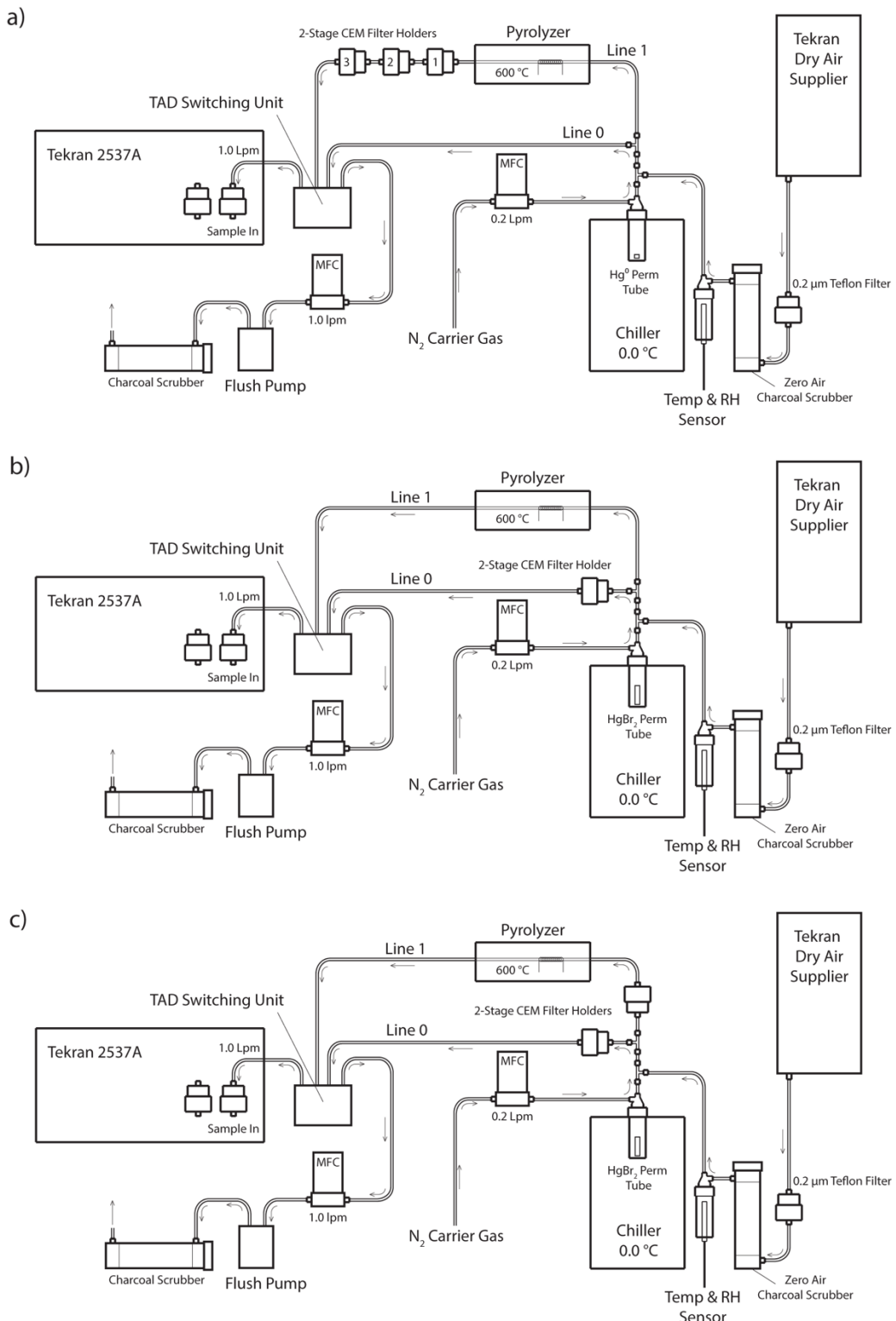
512 Slemr, F., Angot, H., Dommergue, A., Magand, O., Barret, M., Weigelt, A., Ebinghaus, R.,
513 Brunke, E., A Pfaffhuber, K., Edwards, G., Howard, D., Powell, J., Keywood, M., and Wang, F.:
514 Comparison of mercury concentrations measured at several sites in the Southern Hemisphere,
515 3125-3133 pp., 2015.

516 Temme, C., Einax, J. W., Ebinghaus, R., and Schroeder, W. H.: Measurements of Atmospheric
517 Mercury Species at a Coastal Site in the Antarctic and over the South Atlantic Ocean during
518 Polar Summer, Environmental Science & Technology, 37, 22-31, 10.1021/es025884w, 2003.

519 Xiao, Z., Sommar, J., Wei, S., and Lindqvist, O.: Sampling and determination of gas phase
520 divalent mercury in the air using a KCl coated denuder, Fresenius Journal of Analytical
521 Chemistry, 358, 386-391, 1997.

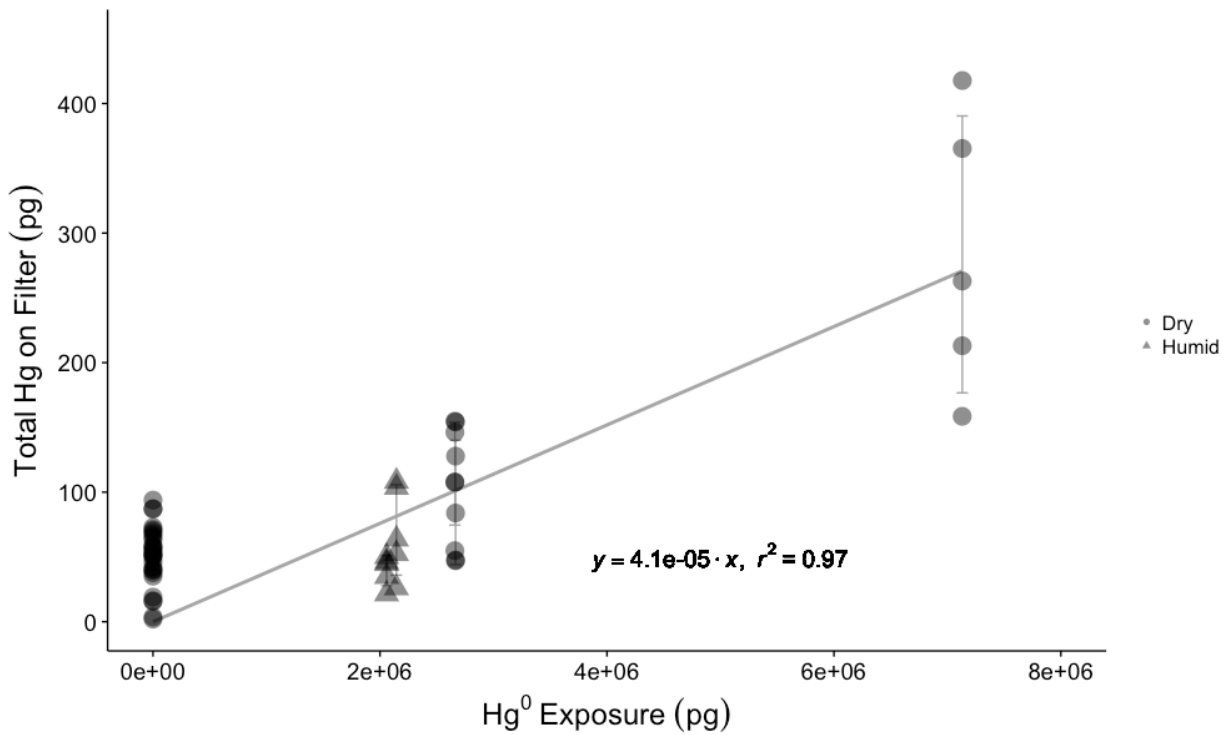
522 Zhang, L., Lyman, S., Mao, H., Lin, C. J., Gay, D. A., Wang, S., Sexauer Gustin, M., Feng, X.,
523 and Wania, F.: A synthesis of research needs for improving the understanding of atmospheric
524 mercury cycling, Atmos. Chem. Phys., 17, 9133-9144, 10.5194/acp-17-9133-2017, 2017.

525



526

527 **Figure 1.** Schematic of the Hg vapor permeation system configurations for: a) GEM permeations b) HgBr_2
 528 permeations c) Simultaneous HgBr_2 loading on two sample lines. Note dry air supplier disconnected for ambient and
 529 elevated humidity HgBr_2 permeations, with sample path starting at 0.2 μm Teflon particulate filter and water bath
 530 inserted immediately in front of the charcoal scrubber. All tubing is PTFE, except for the quartz glass pyrolyzer tube
 531 and PFA filter holders.



532

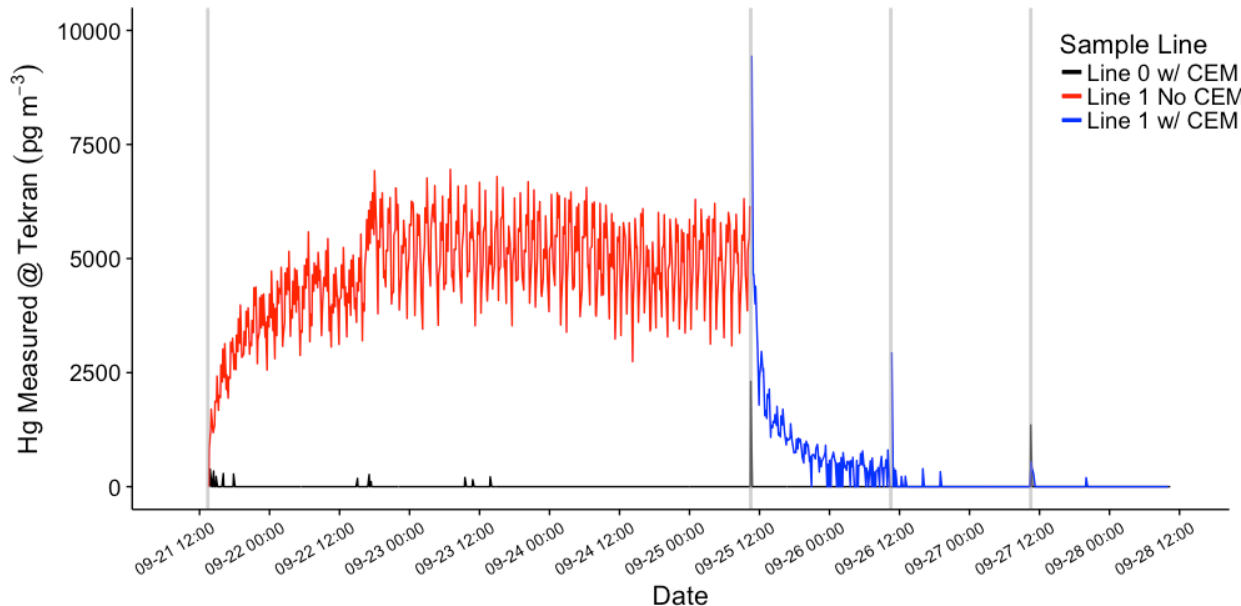
533 **Figure 2.** Total Hg recovered on CEM material for blank filters (Hg exposure = 0 pg) and different Hg⁰ vapor
 534 permeations in dry ($0.5 \pm 0.1 \text{ g m}^{-3}$ WV) and humid air ($2-4 \text{ g m}^{-3}$ WV). Circles represent dry air permeations,
 535 triangles represent humid air exposures, and all permeation exposures were blank-corrected. The regression line
 536 shows the relationship between total Hg⁰ exposure and blank-correct mean total Hg recovered on CEM filters (error
 537 bars \pm one standard deviation), with a slope of 4.1×10^{-5} indicating a linear uptake rate of 0.004%.

538

539

540

541



542
543 **Figure 3.** HgBr₂ permeations in clean dry lab air using the configuration in Figure 1B (red line) and Figure 1C (blue line). The red line indicates total Hg released from permeation tube and passing through pyrolyzer on Line 1 before
544 being measured by Tekran 2537A, black line indicates Hg reaching 2537A through CEM filters on Line 0. Vertical
545 grey lines indicate open system during filter deployments.
546

547

548

549

550

551

552

553

554

555

556

557

558

559

560

Table 1.

Sample	Start	End	Sample Time (min)	Sample Flow (lpm)	Sample Volume (m ³)	Total Hg on CEM (pg)	Blank Correct (pg)	Total Hg @ Tekran (pg)	A to B Filter Brkthru (%)
Mean CEM Filter Blank									
Clean Dry Air (0.3 ± 0.05 g m ⁻³ wv)									
<i>HgBr 1P</i>	9/21/17 13:25	9/25/17 10:25	5580	1.00	5.580	na	na	25181	na
<i>HgBr 1A</i>	9/21/17 13:25	9/25/17 10:25	5580	1.00	5.580	49478	49424		
<i>HgBr 1B</i>						101	47	15	0.10
<i>HgBr 2A</i>	9/25/17 10:30	9/26/17 10:30	1440	1.00	1.440	8901	8847	0	0.20
<i>HgBr 2B</i>						71	17		
<i>HgBr 3A</i>	9/25/17 10:30	9/26/17 10:30	1440	1.00	1.440	9125	9072	1155	0.36
<i>HgBr 3B</i>						86	33		
<i>HgBr 4A</i>	9/26/17 10:40	9/27/17 10:25	1425	1.00	1.425	8494	8440	0	0.28
<i>HgBr 4B</i>						77	24		
<i>HgBr 5A</i>	9/26/17 10:40	9/27/17 10:25	1425	1.00	1.425	8306	8253	10	0.36
<i>HgBr 5B</i>						83	29		
<i>HgBr 6A</i>	9/27/17 10:35	9/28/17 10:25	1430	1.00	1.430	8496	8442	0	0.22
<i>HgBr 6B</i>						72	19		
<i>HgBr 7A</i>	9/27/17 10:35	9/28/17 10:05	1410	1.00	1.410	8386	8333	6	0.15
<i>HgBr 7B</i>						66	13		
Clean Humid Air (4.4 ± .2 g m ⁻³ wv)									
<i>HgBr H1P</i>	10/2/17 16:10	10/3/17 15:20	1390	1.00	1.390	na	na	5888	na
<i>HgBr H1A</i>	10/2/17 16:10	10/3/17 15:20	1390	1.00	1.390	10498	10444	1700	0.25
<i>HgBr H1B</i>						80	27		
<i>HgBr H2A</i>	10/3/17 15:30	10/4/17 14:40	1390	1.00	1.390	8589	8535	164	0.13
<i>HgBr H2B</i>						65	11		
<i>HgBr H3A</i>	10/3/17 15:30	10/4/17 14:40	1390	1.00	1.390	8182	8129	420	0.54
<i>HgBr H3B</i>						98	44		
<i>HgBr H4A</i>	10/4/17 14:50	10/5/17 11:50	1260	1.00	1.260	7504	7451	0	0.31
<i>HgBr H4B</i>						76	23		
<i>HgBr H5A</i>	10/4/17 14:50	10/5/17 11:50	1260	1.00	1.260	7576	7522	25	0.25
<i>HgBr H5B</i>						73	19		
<i>HgBr H6P</i>	10/5/17 12:05	10/9/17 10:25	5660	1.00	5.660	na	na	11889	na
<i>HgBr H7A</i>	10/9/17 10:40	10/10/17 10:45	1445	1.00	1.445	9024	8970	105	na
<i>HgBr H7B</i>						2672*	2618*		
<i>HgBr H8A</i>	10/9/17 10:40	10/10/17 10:45	1445	1.00	1.445	12359	12305	397	na
<i>HgBr H8B</i>						75	21		
Clean High Humidity Air (10.9 ± 1.7 g m ⁻³ wv)									
<i>HgBr H9A</i>	10/10/17 10:50	10/11/17 9:30	1360	1.00	1.360	10920	10866	181	0.22
<i>HgBr H9B</i>						78	24		
<i>HgBr H10A</i>	10/10/17 10:50	10/11/17 9:30	1360	1.00	1.360	11413	11359	308	0.00
<i>HgBr H10B</i>						53	0		
<i>HgBr H11A</i>	10/11/17 9:35	10/12/17 9:35	1440	1.00	1.440	12001	11947	5	0.00
<i>HgBr H11B</i>						52	0		
<i>HgBr H12A</i>	10/11/17 9:35	10/12/17 9:35	1440	1.00	1.440	12579	12525	40	0.29
<i>HgBr H12B</i>						90	36		
<i>HgBr H13P</i>	10/12/17 9:40	10/13/17 9:40	1440	1.00	1.440	na	na	1430	na
<i>HgBr H13A</i>	10/12/17 9:40	10/13/17 9:40	1440	1.00	1.440	13152	13099	4	0.12
<i>HgBr H13B</i>						69	16		

561

562 **Table 1.** Summary of CEM filter loading and breakthrough during HgBr₂ permeations. Samples denoted P indicate
 563 approximate permeation rate check through Line 1 via pyrolyzer and Tekran 2537A, italics indicate filter
 564 deployments on Line 1, and * indicates high values due to leak around first filter seal.